

TextME: Bridging Unseen Modalities Through Text Descriptions

Soyeon Hong¹ Jinchan Kim¹ Jaegook You¹ Seungtaek Choi² Suha Kwak³ Hyunsouk Cho⁴

Abstract

Expanding multimodal representations to novel modalities is constrained by reliance on large-scale paired datasets (e.g., text–image, text–audio, text–3D, text–molecule), which are costly and often infeasible in domains requiring expert annotation such as medical imaging and molecular analysis. We introduce **TextME**, the first text-only modality expansion framework, to the best of our knowledge, projecting diverse modalities into LLM embedding space as a unified anchor. Our approach exploits the geometric structure of pretrained contrastive encoders to enable zero-shot cross-modal transfer using only text descriptions, without paired supervision. We empirically validate that such consistent modality gaps exist across image, video, audio, 3D, X-ray, and molecular domains, demonstrating that text-only training can preserve substantial performance of pretrained encoders. We further show that our framework enables emergent cross-modal retrieval between modality pairs not explicitly aligned during training (e.g., audio-to-image, 3D-to-image). These results establish text-only training as a practical alternative to paired supervision for modality expansion.

1. Introduction

Modality expansion, which aligns heterogeneous data modalities into a unified embedding space, has emerged as a core challenge in multimodal representation learning (Baltrušaitis et al., 2018; Manzoor et al., 2023; Liang et al., 2024; Yuan et al., 2025). Recent approaches leverage large-scale paired datasets to project diverse modalities—such as images, audio, and 3D point clouds—into shared semantic spaces where equivalent content maintains proximity

¹Department of Artificial Intelligence, Ajou University, Suwon, South Korea ²Division of Language & AI, Hankuk University of Foreign Studies, Seoul, Korea ³Graduate School of AI, POSTECH, Pohang, Korea ⁴Department of Software, Ajou University, Suwon, South Korea. Correspondence to: Hyunsouk Cho <hyunsouk@ajou.ac.kr>.

Preprint. February 4, 2026.

	Data Requirement	Training Data Scale	Pretrained Encoder Reuse
ImageBind (CVPR’23), LanguageBind (ICLR’24)	Hard (Bi-modal pairs)	Extremely Large (~1B)	No support (from scratch)
C-MCR (NIPS’23), Ex-MCR (NIPS’24), FreeBind (ICML’24), OmniBind (ICLR’25)	Infeasible (pseudo pairs)	Large (~10M)	Support (Train projectors)
TextME (Ours)	Easy (Unpaired)	Small (~1M)	Support (Train projectors)

Figure 1. Comparison of modality expansion approaches. Unlike prior methods that require large-scale paired data or pseudo-pair construction through overlapping encoders, **TextME** achieves modality expansion using only unpaired text descriptions while reusing pretrained encoders.

(Zhang et al., 2023a; Han et al., 2023; Zhu et al., 2023; Lyu et al., 2024; Guo et al., 2023). While text–image and text–audio corpora have enabled remarkable progress in vision–language (Radford et al., 2021; Jia et al., 2021) and audio–language modeling (Wu et al., 2023; Manco et al., 2022), extending this paradigm to specialized domains proves prohibitively expensive or infeasible. Medical imaging requires costly expert annotations while navigating privacy constraints (Wang et al., 2025; Ziller et al., 2021), molecular analysis demands complex domain-specific representations (Xiao et al., 2024), and 3D modeling necessitates labor-intensive curation (Deitke et al., 2023). Consequently, the scalability of modality expansion remains fundamentally limited by the availability of paired supervision.

Recent methods reduce computational costs by reusing pretrained encoders through lightweight projection networks (Wang et al., 2023b; Zhang et al., 2024b; Wang et al., 2024a;b), yet they still require constructing semantically aligned pseudo pairs across all target modalities through overlapping encoders. Meanwhile, prior work has revealed that contrastive encoders exhibit a consistent modality gap—a systematic offset between text and modality embeddings—that can enable cross-modal transfer via simple geometric operations (Liang et al., 2022; Zhang et al., 2023b; 2024a). However, these studies have primarily focused on analyzing the gap in vision–language models or

mitigating the gap within paired-data settings; whether this geometric property can be exploited to eliminate the need for paired supervision altogether remains unexplored. In addition, there is no guidance on which modalities are amenable to effective alignment and which are not.

In this work, we demonstrate that the modality gap can enable modality expansion without paired supervision. We propose **TextME**, a framework that projects modality-specific embeddings into LLM embedding space as a unified semantic anchor by applying precomputed offset corrections derived from the gap structure. As illustrated in Figure 1, unlike prior methods that require large-scale bi-modal pairs or pseudo-pair construction through overlapping encoders, our proposed framework achieves modality expansion using only unpaired text descriptions—with substantially reduced data requirements while fully leveraging pretrained encoders through lightweight projectors.

We evaluate the framework across six diverse modalities—image, video, audio, 3D point clouds, X-ray, and molecules—on both cross-modal retrieval and zero-shot classification tasks. Our experiments demonstrate that **TextME** achieves competitive performance relative to paired-data methods and, notably, enables emergent cross-modal capabilities between modality pairs never observed during training, such as audio-to-3D and molecule-to-image retrieval. These results suggest that text modality can create meaningful semantic bridges across arbitrary modalities without explicit cross-modal supervision. To better understand the variation in performance across modalities, we further analyze the geometric properties of each encoder and find that the consistency of gap-content orthogonality correlates with downstream performance, providing insight into when text-only expansion is most effective.

Our contribution is three-fold:

- We propose **TextME**, a text-only modality expansion framework that exploits modality gap geometry to learn cross-modal projections using only text descriptions, eliminating the need for paired multimodal supervision during training.
- We investigate LLM embedding space as a unified anchor for modality expansion and compare it against multimodal encoder representations, analyzing their varying effectiveness across tasks and modalities.
- We empirically validate the framework across six diverse modalities, demonstrating competitive performance on retrieval and classification tasks and identifying encoder characteristics that predict when text-only expansion is most effective.

2. Preliminaries

2.1. Problem Formulation

Modality expansion aims to integrate pretrained modality-specific encoders into a unified semantic space where similar concepts maintain proximity regardless of their source modality. Let $\mathcal{M} = \{m_1, \dots, m_k\}$ denote a set of target modalities to be aligned. For each modality $m \in \mathcal{M}$, a pretrained contrastive encoder consists of a text branch $E_m^{\text{text}} : \mathcal{T} \rightarrow \mathbb{R}^{d_m}$ and a modal branch $E_m^{\text{modal}} : \mathcal{X}_m \rightarrow \mathbb{R}^{d_m}$, where \mathcal{T} is the space of text descriptions and \mathcal{X}_m is the input space for modality m . Our objective is to learn projection networks $P_m : \mathbb{R}^{d_m} \rightarrow \mathbb{R}^{d_h}$ that map modal embeddings into a shared d_h -dimensional anchor space.

Existing methods require instance-level paired data $\{(x_i, t_i)\}_{i=1}^N$ of modal inputs $x_i \in \mathcal{X}_m$ and text descriptions $t_i \in \mathcal{T}$ to train cross-modal projections (Han et al., 2023; Zhu et al., 2023; Lyu et al., 2024). Recent approaches connect multiple pretrained encoders via overlapping modalities: given encoders pretrained on modality pairs $(\mathcal{A}, \mathcal{B})$ and $(\mathcal{B}, \mathcal{C})$, they leverage data from the shared modality \mathcal{B} to align encoder spaces, enabling transfer to non-overlapping pairs $(\mathcal{A}, \mathcal{C})$ (Wang et al., 2023b; Zhang et al., 2024b; Wang et al., 2024a;b). This requires modality overlap across all target encoders. In this work, we consider a more practical scenario: learning projection networks independently for each modality using only unpaired text descriptions $\{t_i\}_{i=1}^N$, without requiring cross-encoder alignment or access to target modality samples.

2.2. Modality Gap and Interchangeable Space

Prior work has shown that contrastive encoders trained with objectives such as InfoNCE exhibit a systematic offset between text and modal embedding spaces (Liang et al., 2022; Zhang et al., 2023b; 2024a). For each encoder E_m , the modality gap is characterized by the difference between the centroids of modal and text embeddings:

$$\Delta_m = \mu_m^{\text{modal}} - \mu_m^{\text{text}}, \quad (1)$$

where $\mu_m^{\text{modal}} = \mathbb{E}[E_m^{\text{modal}}(x)]$ and $\mu_m^{\text{text}} = \mathbb{E}[E_m^{\text{text}}(t)]$ denote the expected embeddings over their respective distributions. This gap presents a fundamental challenge for text-only training, as projection networks learned from text embeddings cannot directly transfer to modal embeddings that occupy a different region of the space.

Interchangeable Space via Centering. A key observation from Zhang et al. (2024a) is that this challenge can be addressed through independent centering operations. Consider a semantically matched pair (t, x) with embeddings $e_t = E_m^{\text{text}}(t)$ and $e_x = E_m^{\text{modal}}(x)$. Although these embeddings differ due to the modality gap, subtracting their

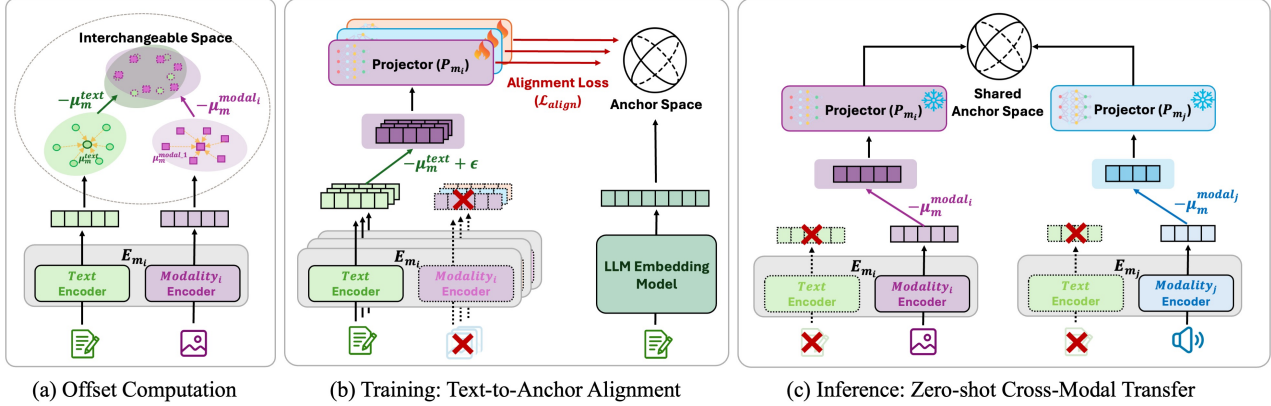


Figure 2. Overview of the TextME pipeline. (a) Offset computation estimates modality-specific centroids from unpaired samples, creating an interchangeable space where centered text and modal embeddings become functionally equivalent. (b) During training, projection networks are learned by aligning centered text embeddings with a unified LLM anchor space, requiring only text descriptions. (c) At inference, centering modal embeddings with the precomputed offset enables zero-shot cross-modal transfer without paired supervision.

respective centroids yields centered embeddings

$$\hat{e}_t = e_t - \mu_m^{\text{text}}, \quad \hat{e}_x = e_x - \mu_m^{\text{modal}}, \quad (2)$$

that satisfy $\hat{e}_t \approx \hat{e}_x$ for semantically corresponding pairs. That is, centering removes the modality-specific bias while preserving the shared semantic content, creating an *interchangeable space* where text and modal embeddings become functionally equivalent (An et al., 2025). This property enables projection networks trained on centered text embeddings to generalize to centered modal embeddings at inference time, forming the basis of our text-only training approach.

3. TextME: Text-only Modality Expansion

We present **TextME**, a framework that enables modality expansion using only text descriptions by exploiting the geometric properties of pretrained contrastive encoders. Figure 2 illustrates the overall pipeline.

3.1. Overview

The key insight of **TextME** is that the interchangeable space described in Section 2 allows projection networks trained on centered text embeddings to generalize to centered modal embeddings at inference time. Our framework operates in two phases. During training, we precompute modality-specific centroids and train lightweight projection networks to map centered text embeddings into a shared anchor space. At inference, we apply the same centering operation to modal embeddings before projection, enabling zero-shot cross-modal transfer without having observed any modal samples during training.

3.2. Offset Computation

As established in Section 2, creating an interchangeable space requires estimating the centroids μ_m^{text} and μ_m^{modal} for each modality. We compute these centroids from representative samples:

$$\mu_m^{\text{text}} = \frac{1}{N} \sum_{i=1}^N E_m^{\text{text}}(t_i), \quad \mu_m^{\text{modal}} = \frac{1}{M} \sum_{j=1}^M E_m^{\text{modal}}(x_j), \quad (3)$$

where $\{t_i\}_{i=1}^N \subset \mathcal{T}$ and $\{x_j\}_{j=1}^M \subset \mathcal{X}_m$ are sampled independently from text and modal distributions. Unlike projection training, these samples need not be instance-level paired—only representative coverage of each distribution is required for accurate centroid estimation.

Importantly, accurate centroid estimation requires only a small number of samples. In our experiments, we find that 5K samples suffice for stable estimation across all evaluated modalities, representing less than 5% of typical paired training requirements (Zhu et al., 2023; Zhang et al., 2024b). The centroids are precomputed once and remain fixed throughout training.

3.3. Text-to-Anchor Alignment

Given the precomputed offsets, we train projection networks using only text descriptions from the target domain. For each modality m , a projection network $P_m : \mathbb{R}^{d_m} \rightarrow \mathbb{R}^{d_m}$ maps centered text embeddings into a shared anchor space.

Anchor Space Selection. We adopt LLM embedding space as our unified anchor rather than multimodal text encoders. While multimodal encoders such as CLIP are optimized for cross-modal matching, LLMs trained on large-scale text corpora capture richer semantic relationships that generalize across diverse domains. To assess cross-domain

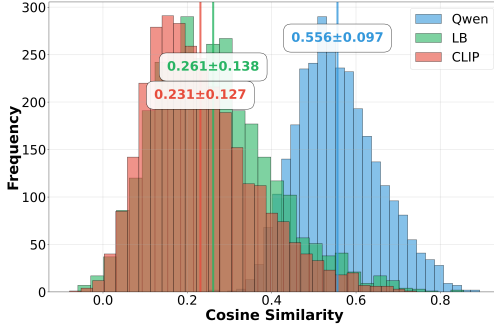


Figure 3. Semantic anchoring comparison. LLM embeddings and multimodal encoders are compared on 3K semantically equivalent cross-modal description pairs. LLM embeddings exhibit clearer separation between matched and unmatched pairs, demonstrating superior cross-domain alignment capability.

alignment capabilities, we analyze 3K audio-image caption pairs from FlickrNet (Senocak et al., 2018), where we generated linguistically distinct but semantically equivalent descriptions using the Gemini API (Google, 2024)—for instance, an image caption “a red sports car speeding on highway” is paired with its audio equivalent “loud engine roar with wind rushing past.” As shown in Figure 3, LLM embeddings (i.e., Qwen) exhibit clearer separation between semantically equivalent and unrelated pairs (0.56 vs. 0.23–0.26 mean cosine similarity) compared to multimodal encoders, suggesting better suitability for bridging heterogeneous descriptions. This advantage is further corroborated by semantic textual similarity benchmarks, where LLM embeddings achieve Spearman correlations of 85–90 compared to 67–68 for multimodal encoders (see Appendix A for details). Based on these findings, we adopt Qwen3-Embedding (Zhang et al., 2025) as our default anchor space.

Training Objective. Given text descriptions $\mathcal{D}_{\text{text}} = \{t_i\}_{i=1}^N$ from the target modality domain, we train the projection network by aligning centered text embeddings with their corresponding LLM embeddings:

$$\mathcal{L}_{\text{align}} = -\frac{1}{B} \sum_{i=1}^B \log \frac{\exp(\text{sim}(z_i, z'_i)/\tau)}{\sum_{j \in \mathcal{N}_i \cup \{i\}} \exp(\text{sim}(z_i, z'_j)/\tau)} \quad (4)$$

where $z_i = P_m(\hat{e}_{t_i})$ is the projected centered text embedding with $\hat{e}_{t_i} = E_m^{\text{text}}(t_i) - \mu_m^{\text{text}}$, $z'_i = E_{\text{LLM}}(t_i)$ is the corresponding LLM embedding, and \mathcal{N}_i contains hard negatives. Following recent language embedding models (Lee et al., 2024; Moreira et al., 2024; Rösch et al., 2024), we employ hard negative mining to focus training on challenging examples near the decision boundary, improving the discriminative quality of learned projections.

3.4. Inference

At inference time, **TextME** enables zero-shot cross-modal transfer by mapping modal embeddings into the interchangeable space. For a non-text input x from modality m , the final embedding is computed as:

$$e_{\text{final}} = P_m(\hat{e}_x) = P_m(E_m^{\text{modal}}(x) - \mu_m^{\text{modal}}). \quad (5)$$

The centering operation transforms the modal embedding into the interchangeable space where text embeddings reside during training. As established in Section 2, centering preserves semantic relationships while removing modality-specific bias, allowing the text-trained projection network P_m to process modal inputs without modification. The final embeddings are thus aligned within the unified LLM anchor space alongside text representations, enabling direct cross-modal retrieval and zero-shot classification.

4. Experiments

We evaluate **TextME** on cross-modal retrieval and zero-shot classification across six modalities: image, video, audio, 3D, X-ray, and molecules. Our experiments address three key questions: (1) whether text-only training can achieve competitive performance relative to paired-data methods and pretrained encoders (Section 4.2); (2) what geometric properties predict success or failure across different modalities (Section 4.3); and (3) how different design choices including anchor space selection and offset correction influence overall performance (Section 4.4).

4.1. Experimental Setup

Modalities and Encoders. We adopt LanguageBind (Zhu et al., 2023) as the text encoder for all text-to-modal retrieval and zero-shot classification tasks. For modal encoders, we adopt CLIP (Radford et al., 2021) for image, ViCLIP (Wang et al., 2023a) for video, CLAP (Elizalde et al., 2023) for audio, Uni3D (Zhou et al., 2023) for 3D, CXR-CLIP (You et al., 2023) for X-ray, and MoleculeSTM (Liu et al., 2023) for molecule. Each encoder pair is independently projected into the shared LLM anchor space for cross-modal matching. We sample 100K text descriptions per modality for projection training, with offset computation on 5K samples.

Baselines. We compare against three categories of methods. First, we report the performance of the original *pre-trained encoders* as reference points. Second, for *paired-data approaches*, we include LanguageBind (Zhu et al., 2023) and Ex-MCR (Zhang et al., 2024b), both of which perform modality expansion using fully-paired multimodal data. Third, for *unpaired-data methods*, we compare with COX[†] (Huang et al., 2025), which learns target modality representations from scratch without instance-level pairing but requires substantial target modality data and classification

Table 1. Zero-shot performance across all evaluation benchmarks. PPR: Performance Preservation Ratio (%) relative to pretrained encoders. \times indicates unavailable results due to missing official implementations or incompatible evaluation protocols. Bold indicates best among unpaired methods. \dagger Our reproduction.

	Text \rightarrow X Retrieval										Classification					Emergent X \rightarrow X		
	Image			Video			Audio		Mol.		Audio		3D		X-ray	A \rightarrow I		
	COCO	Flkr.	MSR.	MSVD	DiDe.	ACaps.	Clo.	Drug.	ASet.	ESC	MN40.	Scan.	RSNA	Flkr.	3D \rightarrow I	Data Requirements		
Pretrained	48.29	77.70	37.00	51.06	31.27	22.47	16.90	79.19	9.32	85.20	67.75	42.21	52.64	\times	\times			
<i>Paired-data methods</i>																		
LanguageBind	44.53	73.42	45.30	65.22	36.85	12.42	11.32	\times	18.33	94.00	\times	\times	\times	1.52	\times	10M pairs		
Ex-MCR	40.24	71.89	\times	\times	\times	19.07	7.01	\times	6.67	71.20	66.53	40.31	\times	1.57	5.67	1M pairs*		
<i>Unpaired-data methods</i>																		
Naïve	0.01	0.04	0.00	0.00	0.00	0.02	0.04	10.17	1.14	2.90	0.81	3.32	26.36	0.02	0.00	0		
COX \dagger	0.02	0.20	5.10	0.00	0.10	0.08	0.11	7.63	1.26	2.00	4.05	2.84	22.53	0.02	0.00	10K labels		
TextME	28.63	51.66	26.40	45.82	24.10	15.35	7.81	34.75	5.80	77.25	70.86	42.15	46.59	1.06	10.27	100K text		
PPR(%)	59.3	66.5	71.4	89.7	77.1	68.3	46.2	43.9	62.2	90.7	104.6	99.9	88.5	\times	\times			

*Indirect: uses overlapping modality from existing MCR spaces. TextME requires **zero paired data** and **zero labeled target data**.

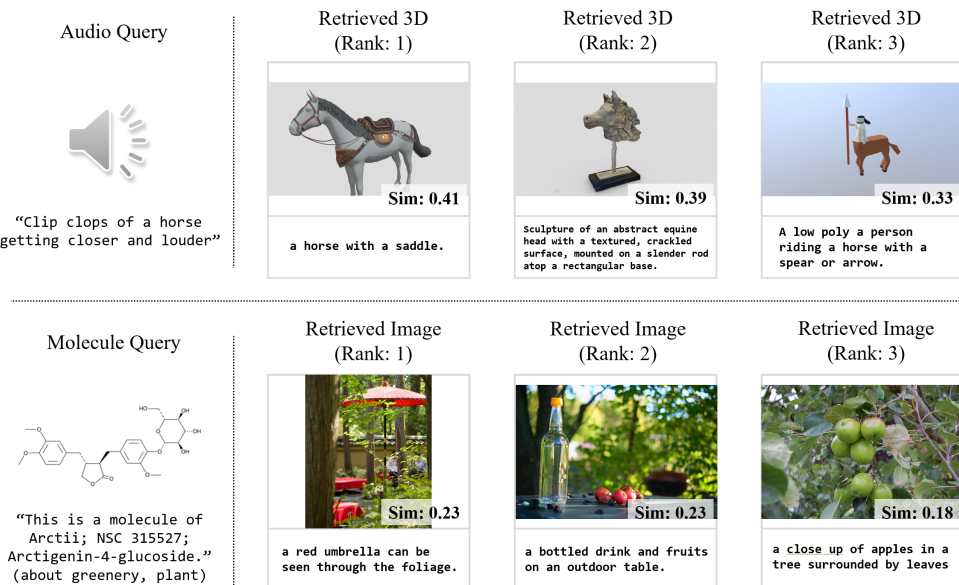


Figure 4. Emergent cross-modal retrieval without paired supervision. Audio queries retrieve semantically related 3D objects (top), and molecular structures retrieve contextually appropriate images (bottom). These modality pairs were never seen during training, demonstrating that text-anchored alignment creates semantic bridges across arbitrary modalities.

labels. We also include a Naïve baseline that simply aligns embedding dimensions via PCA without any learned projection. Unlike COX, **TextME** requires no target modality data during training.

Evaluation. We evaluate on three task categories: Text \rightarrow X retrieval, emergent cross-modal retrieval between unseen modality pairs, and zero-shot classification. Table 1 reports results on representative benchmarks per modality, selected based on prevalence in prior work (Zhu et al., 2023; Zhang et al., 2024b). We report Recall $@k$ (R $@k$) for retrieval, MRR $@k$ for molecule retrieval following Liu et al. (2023), and Top- k accuracy for classification. We define *Performance Preservation Ratio* (PPR) as the percentage of pretrained encoder performance retained by our method:

PPR = (TextME score/Pretrained score) \times 100%. Complete results across all benchmarks appear in Appendix B.

4.2. Does Text-Only Training Preserve Pretrained Performance?

Table 1 reports performance across all evaluation tasks. **TextME** achieves an average of 74.5% PPR across all tasks, with classification at 89.2% consistently outperforming retrieval at 65.3%, suggesting that offset-based alignment preserves categorical boundaries more effectively than fine-grained similarity structure. Among unpaired baselines, COX (Huang et al., 2025) yields substantially lower performance, as it requires a pretrained classifier on labeled target data. Since official implementations are not publicly available, we trained this classifier from scratch on evaluation

data. In contrast, our framework eliminates the need for labeled target data and paired supervision, thereby enabling direct generalization to novel modalities.

Zero-Shot Retrieval and Classification. Across both task categories, **TextME** substantially outperforms unpaired baselines and achieves comparable results to paired-data methods. As reported in the *Data Requirements* column of Table 1, this performance is achieved using only 100K text descriptions, compared to 1–10M paired samples required by methods such as LanguageBind and Ex-MCR. This reduction of over two orders of magnitude in supervision requirements makes modality expansion practical for specialized domains where paired annotation is prohibitively expensive. In terms of task-specific patterns, classification consistently demonstrates higher preservation than retrieval, as categorical discrimination requires only well-separated decision boundaries whereas retrieval demands fine-grained instance-level similarity that is more sensitive to distortions introduced by offset correction. Notably, 3D zero-shot classification surpasses pretrained Uni3D with 104.6% PPR on ModelNet40, while retrieval preservation varies substantially across modalities. We examine the factors underlying these variations in Section 4.3.

Emergent Cross-Modal Capabilities. The unified anchor space additionally enables retrieval between modality pairs not explicitly aligned during training. As reported in the Emergent X→X columns of Table 1, **TextME** outperforms Ex-MCR on 3D→Image despite the latter requiring paired supervision, and achieves comparable performance to paired-data methods on Audio→Image. To qualitatively examine whether the learned representations enable retrieval between modality pairs without any paired annotations, we conduct cross-modal retrieval experiments using independently collected datasets. Specifically, we sample instances from each modality and perform retrieval across disjoint modality pairs such as Audio→3D and Molecule→Image. Figure 4 presents representative results, demonstrating that audio queries retrieve semantically coherent 3D models and molecular queries retrieve contextually relevant images. These findings suggest that text-anchored alignment establishes implicit semantic correspondences without explicit cross-modal supervision.

4.3. When Does Text-Only Expansion Succeed?

We hypothesize that the effectiveness of text-only expansion depends on how well pretrained encoders satisfy the geometric properties underlying modality gap alignment. The results above support this view, revealing substantial variation in performance preservation across modalities—ranging from over 100% for 3D classification to approximately 42% for Molecule retrieval. To investigate this relationship, we

Table 2. Geometric properties of contrastive encoders. (i) intra-modal independence, (ii) gap consistency, (iii) bounded deviation, (iv) gap-content orthogonality. \dagger : weaker satisfaction (>0.1 for (i), <0.96 for (ii)).

Encoder	Mod.	(i)↓	(ii)↑	(iii)↓	(iv)↓
CLIP	Image	.28 \pm .11	.97 \pm .00	.00 \pm .00	.00 \pm .11
ViCLIP	Video	.18 \pm .11	.98 \pm .00	.00 \pm .00	.00 \pm .06
CLAP	Audio	.12 \pm .18	.97 \pm .01	.00 \pm .00	.00 \pm .15
Uni3D	3D	.07 \pm .06	.96 \pm .00	.00 \pm .00	.00 \pm .04
CXR-CLIP	X-ray	.37 \pm .13	.99 \pm .00	.00 \pm .00	.00 \pm .06
MoleculeSTM	Molecule	.01 \pm .19	.78 \pm .05	.00 \pm .00	.00 \pm .18

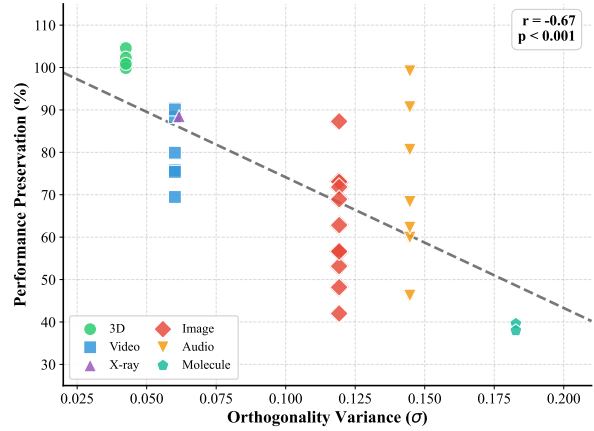


Figure 5. Orthogonality variance vs. performance preservation. Each point represents a single evaluation metric from six modalities, with tasks sharing the same encoder aligned vertically at identical variance values. Lower variance in gap-content orthogonality corresponds to higher downstream performance.

measure the geometric characteristics of each encoder and examine their correlation with downstream performance.

Geometric Properties. Following prior work (Zhang et al., 2024a), we measure four geometric properties for each encoder using 5K paired samples: (i) **Intra-modal independence**: $\mathbb{E}[\cos(\hat{e}, \hat{\mu}_m)]$, measuring whether embeddings are statistically independent from the modality centroid; (ii) **Gap consistency**: $\cos(\Delta_m^{(k)}, \Delta_m)$, measuring whether instance-level offsets $\Delta_m^{(k)} = e_{\text{modal}}^{(k)} - e_{\text{text}}^{(k)}$ align directionally with the group-level offset Δ_m ; (iii) **Bounded deviation**: $\text{std}(\epsilon_k)$ where $\epsilon_k = \Delta_m^{(k)} - \Delta_m$, measuring the variance of instance-level offsets around the mean; (iv) **Gap-content orthogonality**: $|\cos(\Delta_m, r^{(p,q)})|$ where $r^{(p,q)} = e_p - e_q$, measuring whether the modality gap is independent of intra-modal semantic variations. Properties (i) and (ii) ensure that a single offset vector can characterize the modality gap, while (iii) and (iv) ensure that offset correction preserves semantic relationships.

Table 3. Effect of offset correction. Modalities with strong gap consistency benefit substantially, while Molecule with weak consistency shows degradation.

Modality	Benchmark	w/o offset	w/ offset	Δ
3D	ModelNet40	4.05	70.86	+94.30%
3D	ScanObjectNN	5.40	42.15	+87.20%
Audio	AudioCaps	8.68	15.35	+43.50%
Audio	Clotho	4.77	7.81	+38.90%
X-ray	RSNA	31.35	46.59	+32.70%
Molecule	DrugBank	36.44	34.75	-4.60%

Observations. Table 2 demonstrates that all encoders satisfy the requirements for offset-based alignment in expectation. Gap consistency exceeds 0.96 for five of six modalities, and mean orthogonality remains near zero across all encoders, indicating that properties (ii) and (iv) hold on average. However, the degree to which these properties hold at the instance level varies substantially. We find that the variance of property (iv), gap-content orthogonality, serves as a particularly informative predictor of downstream performance. To quantify this relationship, we analyze performance preservation at the individual task level, treating each evaluation metric as a separate observation. This yields 33 data points spanning retrieval benchmarks such as AudioCaps R@1, COCO R@5, and DrugBank MRR, as well as classification benchmarks such as ModelNet40 Top-1 and ESC-50 accuracy. Since tasks evaluated on the same encoder share identical orthogonality variance, they appear vertically aligned in Figure 5. The analysis reveals a moderate negative correlation between orthogonality variance and performance preservation, with Pearson $r = -0.67$ and $p < 0.001$. Encoders exhibiting lower variance in property (iv), notably Uni3D at ± 0.04 and ViCLIP at ± 0.06 , achieve preservation rates consistently above 80%, whereas those with higher variance such as CLAP at ± 0.15 and MoleculeSTM at ± 0.18 show greater performance degradation. This pattern suggests that inconsistent orthogonality introduces variable distortions during offset correction, with fine-grained retrieval tasks affected more severely than categorical classification. We additionally note that MoleculeSTM exhibits a distinct failure mode in property (ii), as its gap consistency of only 0.78 indicates that a single offset vector inadequately characterizes the modality gap for molecular embeddings.

4.4. How Do Design Choices Affect Performance?

Effect of Offset Correction. Table 3 examines the contribution of offset correction across modalities with varying gap consistency. For modalities satisfying strong gap consistency above 0.95, offset correction yields substantial improvements, with 3D classification increasing from 4.05% to 70.86% on ModelNet40 and Audio retrieval improving by 43.5% on AudioCaps. In contrast, Molecule with gap

Table 4. Anchor space comparison. LLM-based anchors yield stronger Text→X retrieval performance, while multimodal anchors achieve comparable results on classification.

Anchor	Retrieval			Classification		
	AudioCaps R@1	Clotho R@1	DrugBank MRR	3D Top-1	Audio Top-1	X-ray Top-1
<i>Multimodal encoders</i>						
CLIP	15.91	6.60	36.44	78.04	86.70	48.31
LanguageBind	14.54	6.93	29.66	81.12	74.65	44.99
<i>LLM embedding models</i>						
NV-Embed-v2	16.20	7.75	26.27	76.30	79.40	48.59
Qwen3-Embed	15.35	7.81	34.75	70.86	77.25	46.59

Table 5. Effect of training data source. Domain-specific captions substantially outperform general-purpose text across all modalities.

Training Data	Audio R@1	3D Top-1	X-ray Top-1	Mol. MRR
all-NLI	6.36	12.10	22.48	16.10
Domain captions	15.35	70.86	46.59	34.75
Improvement	+141%	+485%	+107%	+116%

consistency of only 0.78 exhibits a slight performance degradation of 4.6%, indicating that unreliable offset estimation can introduce harmful distortions. These results suggest that practitioners should verify gap consistency before applying geometric alignment.

Anchor Space Selection. Table 4 compares two categories of anchor spaces, which are LLM embeddings and multimodal encoders. The results reveal a task-dependent pattern in anchor space effectiveness. For retrieval tasks, LLM-based anchors such as NV-Embed-v2 and Qwen3-Embedding consistently outperform multimodal encoders on audio benchmarks, achieving 16.20 and 15.35 R@1 on AudioCaps compared to 14.54–15.91 for multimodal anchors. We attribute this advantage to the semantic representations acquired through large-scale language pretraining, which capture fine-grained similarity relationships required for retrieval. For classification tasks, multimodal anchors such as CLIP and LanguageBind demonstrate superior performance, with CLIP achieving 86.70 on Audio and LanguageBind achieving 81.12 on 3D modality. We attribute this advantage to the discriminative decision boundaries acquired through vision-language contrastive training. Based on these findings, we adopt Qwen3-Embedding as the default anchor space, as it provides balanced performance across retrieval and classification.

Training Data Source. To validate whether general-purpose text corpora that have never been associated with any target modality can enable cross-modal transfer, we train projection networks using all-NLI, a corpus combining MNLI (Williams et al., 2018) and SNLI (Bowman

et al., 2015) with 100K sentence pairs, following the previous work of text-only training (Xiao et al., 2025). Table 5 presents the results. Training on all-NLI yields substantially lower performance compared to domain-specific captions across all modalities, with the degradation being most pronounced for 3D, which drops from 70.86% to 12.10%. This performance gap reflects the distributional mismatch between general linguistic expressions and the specialized vocabularies characteristic of each modality domain. Nevertheless, the non-trivial cross-modal transfer achieved with general-purpose text validates our text-only training paradigm. A systematic analysis of how distributional characteristics such as domain coverage and vocabulary specificity influence alignment quality presents a promising avenue for developing more refined data selection strategies.

5. Related Work

Modality Expansion. Contrastive learning has enabled effective multimodal alignment by projecting different modalities into shared semantic spaces (Radford et al., 2021; Jia et al., 2021). Subsequent work extends this paradigm to multiple modalities through central hubs: ImageBind (Girdhar et al., 2023) uses images as the anchor modality, while LanguageBind (Zhu et al., 2023) leverages text for broader semantic coverage. To reduce computational costs, recent methods connect frozen pretrained encoders through lightweight projectors. C-MCR (Wang et al., 2023b) and Ex-MCR (Zhang et al., 2024b) learn adapters between encoder pairs, while FreeBind (Wang et al., 2024a) and OmniBind (Wang et al., 2024b) ensemble multiple encoders per modality. However, all these approaches require instance-level paired supervision during training, which becomes prohibitive in specialized domains where paired data is scarce. **TextME** eliminates this requirement through text-only training of projection networks.

Modality Gap Analysis. The modality gap—a systematic offset between text and non-text embeddings in contrastive models—was first identified by Liang et al. (2022), who characterized its geometric structure in CLIP. Subsequent work has sought to understand this phenomenon from multiple perspectives, including linear separability analysis (Shi et al., 2023), double-ellipsoid geometry (Levi & Gilboa, 2024), and the distinction between modality-specific and contrastive components (Fahim et al., 2024). Building on these insights, several methods exploit the gap for downstream applications such as vision model diagnosis (Zhang et al., 2023b) and cross-modal transfer via zero-centering (Zhang et al., 2024a). More recent efforts focus on mitigating the gap through learnable correction models (Park et al., 2024; Eslami & de Melo, 2024), embedding standardization (An et al., 2025), or centroid alignment for

mixed-modality retrieval (Li et al., 2025). However, these methods operate in paired-data settings and focus on improving alignment within existing modality pairs. While prior work has primarily analyzed the gap in vision-language models, we demonstrate that this geometric property generalizes across six diverse modalities—including 3D, X-ray, and molecules—and can be exploited for modality expansion without paired supervision.

LLM-Anchored Multimodal Learning. Recent work leverages LLMs as semantic anchors for multimodal alignment, exploiting their broad semantic coverage and contextual understanding acquired through large-scale language pretraining. Generative approaches integrate LLMs with multimodal encoders for instruction tuning (Han et al., 2023) and unified cross-modal generation (Han et al., 2024). Representation-focused methods include UniBind (Lyu et al., 2024), which creates LLM-augmented unified spaces, and LLM2CLIP (Huang et al., 2024), which enhances dense caption understanding through large-scale paired training on tens of millions of image-caption pairs. More recently, E5-V (Jiang et al., 2024) and LCO-Emb (Xiao et al., 2025) show that text-only contrastive learning can enhance MLLM embedding quality without multimodal training data. However, these methods operate within unified MLLM architectures where cross-modal alignment is implicitly established during generative pretraining. In contrast, **TextME** addresses the alignment of independently trained contrastive encoders with architecturally heterogeneous embedding spaces, enabling expansion to specialized domains such as 3D, X-ray, and molecules without requiring a shared backbone.

6. Conclusion

We introduced **TextME**, a framework that leverages the consistent modality gap in pretrained contrastive encoders to enable text-only modality expansion. By projecting diverse modalities into LLM embedding space as a unified anchor, our approach preserves substantial performance of pretrained encoders across six modalities using only text descriptions for projection learning. Compared to existing paired-data methods, **TextME** reduces data requirements by over 95% while eliminating the need for paired multimodal supervision. Furthermore, the framework enables emergent cross-modal retrieval between modality pairs never seen during training (e.g., audio-to-image, 3D-to-image), demonstrating that text-anchored alignment can establish implicit correspondences across arbitrary modalities without direct cross-modal pairing. These results suggest that text-only training offers a practical pathway for integrating specialized modalities—such as medical imaging and molecular structures—into unified multimodal systems without the prohibitive cost of expert annotation.

Impact Statement

This work aims to reduce the data annotation burden in multimodal learning, potentially democratizing access to multimodal AI systems in specialized domains such as medical imaging and molecular analysis where paired supervision is prohibitively expensive. While this could accelerate beneficial applications in healthcare and drug discovery, practitioners should exercise appropriate caution when deploying such models in safety-critical settings, ensuring thorough validation before clinical or real-world use. We do not foresee immediate negative societal consequences beyond those common to advances in representation learning.

References

An, N. M., Kim, E., Thorne, J., and Shim, H. IoT: Embedding standardization method towards zero modality gap. In *Proceedings of the 63rd Annual Meeting of the Association for Computational Linguistics (Volume 1: Long Papers)*, pp. 27182–27199, 2025.

Anne Hendricks, L., Wang, O., Shechtman, E., Sivic, J., Darrell, T., and Russell, B. Localizing moments in video with natural language. In *Proceedings of the IEEE international conference on computer vision*, pp. 5803–5812, 2017.

Baltrušaitis, T., Ahuja, C., and Morency, L.-P. Multimodal machine learning: A survey and taxonomy. *IEEE transactions on pattern analysis and machine intelligence*, 41(2):423–443, 2018.

Bowman, S., Angeli, G., Potts, C., and Manning, C. D. A large annotated corpus for learning natural language inference. In *Proceedings of the 2015 conference on empirical methods in natural language processing*, pp. 632–642, 2015.

Chen, D. and Dolan, W. B. Collecting highly parallel data for paraphrase evaluation. In *Proceedings of the 49th annual meeting of the association for computational linguistics: human language technologies*, pp. 190–200, 2011.

Deitke, M., Schwenk, D., Salvador, J., Weihs, L., Michel, O., VanderBilt, E., Schmidt, L., Ehsani, K., Kembhavi, A., and Farhadi, A. Objaverse: A universe of annotated 3d objects. In *Proceedings of the IEEE/CVF conference on computer vision and pattern recognition*, pp. 13142–13153, 2023.

Drossos, K., Lipping, S., and Virtanen, T. Clotho: An audio captioning dataset. In *ICASSP 2020-2020 IEEE International Conference on Acoustics, Speech and Signal Processing (ICASSP)*, pp. 736–740. IEEE, 2020.

Elizalde, B., Deshmukh, S., Al Ismail, M., and Wang, H. Clap learning audio concepts from natural language supervision. In *ICASSP 2023-2023 IEEE International Conference on Acoustics, Speech and Signal Processing (ICASSP)*, pp. 1–5. IEEE, 2023.

Eslami, S. and de Melo, G. Mitigate the gap: Investigating approaches for improving cross-modal alignment in clip. *arXiv preprint arXiv:2406.17639*, 2024.

Fahim, A., Murphy, A., and Fyshe, A. It’s not a modality gap: Characterizing and addressing the contrastive gap. *arXiv preprint arXiv:2405.18570*, 2024.

Gemmeke, J. F., Ellis, D. P., Freedman, D., Jansen, A., Lawrence, W., Moore, R. C., Plakal, M., and Ritter, M. Audio set: An ontology and human-labeled dataset for audio events. In *2017 IEEE international conference on acoustics, speech and signal processing (ICASSP)*, pp. 776–780. IEEE, 2017.

Girdhar, R., El-Nouby, A., Liu, Z., Singh, M., Alwala, K. V., Joulin, A., and Misra, I. Imagebind: One embedding space to bind them all. In *Proceedings of the IEEE/CVF conference on computer vision and pattern recognition*, pp. 15180–15190, 2023.

Google. Gemini api, 2024. URL <https://ai.google.dev/gemini-api>. Accessed: January 2025.

Guo, Z., Zhang, R., Zhu, X., Tang, Y., Ma, X., Han, J., Chen, K., Gao, P., Li, X., Li, H., et al. Point-bind & point-llm: Aligning point cloud with multi-modality for 3d understanding, generation, and instruction following. *arXiv preprint arXiv:2309.00615*, 2023.

Han, J., Zhang, R., Shao, W., Gao, P., Xu, P., Xiao, H., Zhang, K., Liu, C., Wen, S., Guo, Z., et al. Imagebind-llm: Multi-modality instruction tuning. *arXiv preprint arXiv:2309.03905*, 2023.

Han, J., Gong, K., Zhang, Y., Wang, J., Zhang, K., Lin, D., Qiao, Y., Gao, P., and Yue, X. Onellm: One framework to align all modalities with language. In *Proceedings of the IEEE/CVF Conference on Computer Vision and Pattern Recognition*, pp. 26584–26595, 2024.

Huang, W., Wu, A., Yang, Y., Luo, X., Yang, Y., Hu, L., Dai, Q., Wang, C., Dai, X., Chen, D., et al. Llm2clip: Powerful language model unlocks richer visual representation. *arXiv preprint arXiv:2411.04997*, 2024.

Huang, Z., Niu, G., Han, B., Sugiyama, M., and Liu, T. Towards out-of-modal generalization without instance-level modal correspondence. In *The Thirteenth International Conference on Learning Representations*, 2025.

Irvin, J., Rajpurkar, P., Ko, M., Yu, Y., Ciurea-Ilcus, S., Chute, C., Marklund, H., Haghgoor, B., Ball, R., Shpan-skaya, K., et al. Chexpert: A large chest radiograph dataset with uncertainty labels and expert comparison. In *Proceedings of the AAAI conference on artificial intelligence*, volume 33, pp. 590–597, 2019.

Jia, C., Yang, Y., Xia, Y., Chen, Y.-T., Parekh, Z., Pham, H., Le, Q., Sung, Y.-H., Li, Z., and Duerig, T. Scaling up visual and vision-language representation learning with noisy text supervision. In *International conference on machine learning*, pp. 4904–4916. PMLR, 2021.

Jiang, T., Song, M., Zhang, Z., Huang, H., Deng, W., Sun, F., Zhang, Q., Wang, D., and Zhuang, F. E5-v: Universal embeddings with multimodal large language models. *arXiv preprint arXiv:2407.12580*, 2024.

Kim, C. D., Kim, B., Lee, H., and Kim, G. Audiocaps: Generating captions for audios in the wild. In *Proceedings of the 2019 Conference of the North American Chapter of the Association for Computational Linguistics: Human Language Technologies, Volume 1 (Long and Short Papers)*, pp. 119–132, 2019.

Kim, S., Chen, J., Cheng, T., Gindulyte, A., He, J., He, S., Li, Q., Shoemaker, B. A., Thiessen, P. A., Yu, B., et al. Pubchem 2025 update. *Nucleic acids research*, 53(D1):D1516–D1525, 2025.

Knox, C., Wilson, M., Klinger, C. M., Franklin, M., Oler, E., Wilson, A., Pon, A., Cox, J., Chin, N. E., Strawbridge, S. A., et al. Drugbank 6.0: the drugbank knowledgebase for 2024. *Nucleic acids research*, 52(D1):D1265–D1275, 2024.

Lee, C., Roy, R., Xu, M., Raiman, J., Shoeybi, M., Catan-zaro, B., and Ping, W. Nv-embed: Improved techniques for training llms as generalist embedding models. *arXiv preprint arXiv:2405.17428*, 2024.

Levi, M. Y. and Gilboa, G. The double-ellipsoid geometry of clip. *arXiv preprint arXiv:2411.14517*, 2024.

Li, B., Zhang, Y., Wang, X., Liang, W., Schmidt, L., and Yeung-Levy, S. Closing the modality gap for mixed modality search. *arXiv preprint arXiv:2507.19054*, 2025.

Liang, P. P., Zadeh, A., and Morency, L.-P. Foundations & trends in multimodal machine learning: Principles, challenges, and open questions. *ACM Computing Surveys*, 56(10):1–42, 2024.

Liang, V. W., Zhang, Y., Kwon, Y., Yeung, S., and Zou, J. Y. Mind the gap: Understanding the modality gap in multi-modal contrastive representation learning. *Advances in Neural Information Processing Systems*, 35: 17612–17625, 2022.

Lin, T.-Y., Maire, M., Belongie, S., Hays, J., Perona, P., Ra-manan, D., Dollár, P., and Zitnick, C. L. Microsoft coco: Common objects in context. In *European conference on computer vision*, pp. 740–755. Springer, 2014.

Liu, S., Nie, W., Wang, C., Lu, J., Qiao, Z., Liu, L., Tang, J., Xiao, C., and Anandkumar, A. Multi-modal molecule structure–text model for text-based retrieval and editing. *Nature Machine Intelligence*, 5(12):1447–1457, 2023.

Lyu, Y., Zheng, X., Zhou, J., and Wang, L. Unibind: Llm-augmented unified and balanced representation space to bind them all. In *Proceedings of the IEEE/CVF Conference on Computer Vision and Pattern Recognition*, pp. 26752–26762, 2024.

Manco, I., Benetos, E., Quinton, E., and Fazekas, G. Contrastive audio-language learning for music. *arXiv preprint arXiv:2208.12208*, 2022.

Manzoor, M. A., Albarri, S., Xian, Z., Meng, Z., Nakov, P., and Liang, S. Multimodality representation learning: A survey on evolution, pretraining and its applications. *ACM Transactions on Multimedia Computing, Communica-tions and Applications*, 20(3):1–34, 2023.

Moreira, G. d. S. P., Osmulski, R., Xu, M., Ak, R., Schif-ferer, B., and Oldridge, E. Nv-retriever: Improving text embedding models with effective hard-negative mining. *arXiv preprint arXiv:2407.15831*, 2024.

Park, J., Lee, J., and Sohn, K. Bridging vision and lan-guage spaces with assignment prediction. *arXiv preprint arXiv:2404.09632*, 2024.

Piczkak, K. J. Esc: Dataset for environmental sound classification. In *Proceedings of the 23rd ACM international conference on Multimedia*, pp. 1015–1018, 2015.

Plummer, B. A., Wang, L., Cervantes, C. M., Caicedo, J. C., Hockenmaier, J., and Lazebnik, S. Flickr30k entities: Collecting region-to-phrase correspondences for richer image-to-sentence models. In *Proceedings of the IEEE international conference on computer vision*, pp. 2641–2649, 2015.

Radford, A., Kim, J. W., Hallacy, C., Ramesh, A., Goh, G., Agarwal, S., Sastry, G., Askell, A., Mishkin, P., Clark, J., et al. Learning transferable visual models from natural language supervision. In *International conference on machine learning*, pp. 8748–8763. PmLR, 2021.

Rösch, P. J., Oswald, N., Geierhos, M., and Libovický, J. Enhancing conceptual understanding in multimodal contrastive learning through hard negative samples. *arXiv preprint arXiv:2403.02875*, 2024.

RSNA. RSNA Pneumonia Detection Challenge. <https://www.kaggle.com/competitions/rsna-pneumonia-detection-challenge>, 2018. [Online; accessed 28-Aug-2018].

Senocak, A., Oh, T.-H., Kim, J., Yang, M.-H., and Kweon, I. S. Learning to localize sound source in visual scenes. In *Proceedings of the IEEE conference on computer vision and pattern recognition*, pp. 4358–4366, 2018.

Shi, P., Welle, M. C., Björkman, M., and Krägic, D. Towards understanding the modality gap in clip. In *ICLR 2023 workshop on multimodal representation learning: perks and pitfalls*, 2023.

Sun, J., Zhang, Q., Kailkhura, B., Yu, Z., Xiao, C., and Mao, Z. M. Benchmarking robustness of 3d point cloud recognition against common corruptions. *arXiv preprint arXiv:2201.12296*, 2022.

Uy, M. A., Pham, Q.-H., Hua, B.-S., Nguyen, T., and Yeung, S.-K. Revisiting point cloud classification: A new benchmark dataset and classification model on real-world data. In *Proceedings of the IEEE/CVF international conference on computer vision*, pp. 1588–1597, 2019.

Wang, X., Wang, F., Li, Y., Ma, Q., Wang, S., Jiang, B., and Tang, J. Cxpmrg-bench: Pre-training and benchmarking for x-ray medical report generation on cheexpert plus dataset. In *Proceedings of the Computer Vision and Pattern Recognition Conference*, pp. 5123–5133, 2025.

Wang, Y., He, Y., Li, Y., Li, K., Yu, J., Ma, X., Li, X., Chen, G., Chen, X., Wang, Y., et al. Internvid: A large-scale video-text dataset for multimodal understanding and generation. *arXiv preprint arXiv:2307.06942*, 2023a.

Wang, Z., Zhao, Y., Huang, H., Liu, J., Yin, A., Tang, L., Li, L., Wang, Y., Zhang, Z., and Zhao, Z. Connecting multi-modal contrastive representations. *Advances in Neural Information Processing Systems*, 36:22099–22114, 2023b.

Wang, Z., Zhang, Z., Cheng, X., Huang, R., Liu, L., Ye, Z., Huang, H., Zhao, Y., Jin, T., Gao, P., et al. Freebind: Free lunch in unified multimodal space via knowledge fusion. *arXiv preprint arXiv:2405.04883*, 2024a.

Wang, Z., Zhang, Z., Zhang, H., Liu, L., Huang, R., Cheng, X., Zhao, H., and Zhao, Z. Omnibind: Large-scale omni multimodal representation via binding spaces. *arXiv preprint arXiv:2407.11895*, 2024b.

Williams, A., Nangia, N., and Bowman, S. A broad-coverage challenge corpus for sentence understanding through inference. In *Proceedings of the 2018 conference of the North American chapter of the association for computational linguistics: human language technologies, volume 1 (long papers)*, pp. 1112–1122, 2018.

Wu, Y., Chen, K., Zhang, T., Hui, Y., Berg-Kirkpatrick, T., and Dubnov, S. Large-scale contrastive language-audio pretraining with feature fusion and keyword-to-caption augmentation. In *ICASSP 2023-2023 IEEE International Conference on Acoustics, Speech and Signal Processing (ICASSP)*, pp. 1–5. IEEE, 2023.

Xiao, C., Chan, H. P., Zhang, H., Xu, W., Aljunied, M., and Rong, Y. Scaling language-centric omnimodal representation learning. *arXiv preprint arXiv:2510.11693*, 2025.

Xiao, T., Cui, C., Zhu, H., and Honavar, V. G. Molbind: Multimodal alignment of language, molecules, and proteins. *arXiv preprint arXiv:2403.08167*, 2024.

Xu, J., Mei, T., Yao, T., and Rui, Y. Msr-vtt: A large video description dataset for bridging video and language. In *Proceedings of the IEEE conference on computer vision and pattern recognition*, pp. 5288–5296, 2016.

You, K., Gu, J., Ham, J., Park, B., Kim, J., Hong, E. K., Baek, W., and Roh, B. Cxr-clip: Toward large scale chest x-ray language-image pre-training. In *International Conference on Medical Image Computing and Computer-Assisted Intervention*, pp. 101–111. Springer, 2023.

Yuan, Y., Li, Z., and Zhao, B. A survey of multimodal learning: Methods, applications, and future. *ACM Computing Surveys*, 57(7):1–34, 2025.

Zhang, Y., Gong, K., Zhang, K., Li, H., Qiao, Y., Ouyang, W., and Yue, X. Meta-transformer: A unified framework for multimodal learning. *arXiv preprint arXiv:2307.10802*, 2023a.

Zhang, Y., HaoChen, J. Z., Huang, S.-C., Wang, K.-C., Zou, J., and Yeung, S. Diagnosing and rectifying vision models using language. *arXiv preprint arXiv:2302.04269*, 2023b.

Zhang, Y., Sui, E., and Yeung-Levy, S. Connect, collapse, corrupt: Learning cross-modal tasks with uni-modal data. *arXiv preprint arXiv:2401.08567*, 2024a.

Zhang, Y., Li, M., Long, D., Zhang, X., Lin, H., Yang, B., Xie, P., Yang, A., Liu, D., Lin, J., et al. Qwen3 embedding: Advancing text embedding and reranking through foundation models. *arXiv preprint arXiv:2506.05176*, 2025.

Zhang, Z., Wang, Z., Liu, L., Huang, R., Cheng, X., Ye, Z., Liu, H., Huang, H., Zhao, Y., Jin, T., et al. Extending multi-modal contrastive representations. *Advances in Neural Information Processing Systems*, 37:91880–91903, 2024b.

Zhou, J., Wang, J., Ma, B., Liu, Y.-S., Huang, T., and Wang, X. Uni3d: Exploring unified 3d representation at scale. *arXiv preprint arXiv:2310.06773*, 2023.

Zhu, B., Lin, B., Ning, M., Yan, Y., Cui, J., Wang, H.,
Pang, Y., Jiang, W., Zhang, J., Li, Z., et al. Language-
bind: Extending video-language pretraining to n-modality
by language-based semantic alignment. *arXiv preprint*
arXiv:2310.01852, 2023.

Ziller, A., Usynin, D., Braren, R., Makowski, M., Rueck-
ert, D., and Kaissis, G. Medical imaging deep learning
with differential privacy. *Scientific Reports*, 11(1):13524,
2021.

A. Semantic Textual Similarity Benchmark Analysis

To validate our choice of LLM embeddings as the semantic anchor space, we conduct comprehensive evaluation on the Semantic Textual Similarity (STS) benchmark suite. Table 6 presents Spearman correlation scores across six STS tasks (STS12–16 and STSBenchmark) comparing multimodal encoders (CLIP (Radford et al., 2021), LanguageBind (Zhu et al., 2023)) against LLM embedding models (NV-Embed-v2 (Lee et al., 2024), Qwen3-Embedding variants (Zhang et al., 2025)).

Table 6. Semantic Textual Similarity (STS) benchmark performance. Spearman correlation (ρ) scores across six STS tasks are reported, comparing multimodal encoders and LLM embedding models.

Model	STS Tasks (Spearman ρ)						Avg.
	STS12	STS13	STS14	STS15	STS16	STSBench	
<i>Multimodal Encoders</i>							
CLIP	61.87	63.83	62.09	76.82	72.89	72.26	68.29
LanguageBind	63.12	67.46	63.27	73.82	73.73	71.60	68.83
<i>LLM Embedding Models</i>							
NV-Embed-v2	77.89	88.30	84.30	89.04	86.77	88.41	85.79
Qwen3-Embed-0.6B	79.35	87.31	79.81	87.28	87.07	86.51	84.56
Qwen3-Embed-4B	84.31	93.20	88.61	92.31	92.07	91.92	90.40

B. Extended Experimental Results

This appendix provides comprehensive experimental results that supplement the main findings in Section 4. We report detailed metrics across all evaluation benchmarks to enable thorough comparison and reproducibility.

B.1. Evaluation Benchmarks

Table 7 provides a complete overview of all evaluation benchmarks. In the main text (Table 1), we report representative benchmarks per modality for clarity: Flickr30k for image, MSVD for video, AudioCaps for audio, and DrugBank for molecule retrieval; ESC-50, ModelNet40, ScanObjectNN, and RSNA for classification.

Table 7. Complete evaluation benchmarks. All datasets used for retrieval and classification tasks are organized by task type and target modality.

Task	Modality	Datasets
Text→X Retrieval	Image	COCO (Lin et al., 2014), Flickr30k (Plummer et al., 2015)
	Video	MSRVTT (Xu et al., 2016), MSVD (Chen & Dolan, 2011), DiDeMo (Anne Hendricks et al., 2017)
	Audio	AudioCaps (Kim et al., 2019), Clotho (Drossos et al., 2020)
	Molecule	DrugBank (Knox et al., 2024)
Emergent X→X	Audio→Image	FlickrNet (Senocak et al., 2018)
	3D→Image	Objaverse (Deitke et al., 2023)
Zero-shot Cls.	3D	ModelNet40 (Sun et al., 2022), ScanObjectNN (Uy et al., 2019)
	Audio	AudioSet (Gemmeke et al., 2017), ESC-50 (Piczak, 2015)
	X-ray	RSNA (RSNA, 2018)

B.2. Detailed Cross-Modal Retrieval Performance

Table 1 in the main text reports representative R@1 metrics for brevity. Here, we provide complete retrieval results including R@5 metrics, which capture whether relevant items appear within the top-5 retrieved candidates. This relaxed criterion is particularly informative for assessing approximate semantic alignment quality.

As shown in Table 8, TextME consistently achieves higher PPR on R@5 compared to R@1 across all benchmarks (e.g., 75.6% vs. 59.3% on COCO, 98.4% vs. 89.7% on MSVD). This pattern indicates that text-only training effectively preserves coarse-grained semantic structure, with the performance gap primarily arising from fine-grained ranking precision. Notably, on MSVD, TextME achieves near-perfect R@5 preservation (98.4%), suggesting that the learned projections successfully capture the underlying semantic relationships for video-text alignment.

Table 8. Detailed Text→Image and Text→Video retrieval performance. R@1 and R@5 metrics are reported. PPR denotes Performance Preservation Ratio (%) relative to pretrained encoders (CLIP for Image, ViCLIP for Video).

	Image Retrieval				Video Retrieval			
	COCO		Flickr30k		MSRVTT		MSVD	
	R@1	R@5	R@1	R@5	R@1	R@5	R@1	R@5
Pretrained	48.29	72.51	77.70	94.16	37.00	63.70	51.06	78.29
TextME	28.63	54.81	51.66	77.90	26.40	50.50	45.82	77.01
PPR (%)	59.3	75.6	66.5	82.7	71.4	79.3	89.7	98.4

Table 9. Detailed Text→Audio and Text→Molecule retrieval performance. R@1 and R@5 metrics are reported for audio, and MRR@10 and MRR@20 for molecule retrieval. PPR denotes Performance Preservation Ratio (%) relative to pretrained encoders (CLAP for Audio, MoleculeSTM for Molecule).

	Audio Retrieval				Molecule Retrieval	
	AudioCaps		Clotho		DrugBank	
	R@1	R@5	R@1	R@5	MRR@10	MRR@20
Pretrained	22.47	54.43	16.90	39.75	79.19	69.17
TextME	15.35	43.88	7.81	23.81	34.75	27.97
PPR (%)	68.3	80.6	46.2	59.9	43.9	40.4

The audio retrieval results exhibit a similar trend, with R@5 preservation consistently exceeding R@1. However, the molecule retrieval task shows lower overall preservation rates, which we attribute to the highly specialized vocabulary in chemical descriptions that differs substantially from the general text distributions used in LLM pretraining.

B.3. Detailed Zero-shot Classification Results

Table 10 provides complete zero-shot classification results including Top-5 accuracy.

Table 10. Detailed zero-shot classification performance. Top-1 and Top-5 accuracy are reported across audio (ESC-50) and 3D (ModelNet40, ScanObjectNN) modalities, along with mAP for AudioSet. PPR denotes Performance Preservation Ratio (%) relative to pretrained encoders.

Method	AudioSet mAP	ESC-50		ModelNet40		ScanObjectNN	
		Top-1	Top-5	Top-1	Top-5	Top-1	Top-5
Pretrained	9.32	85.20	97.70	67.75	90.07	42.21	77.23
LanguageBind	18.33	94.00	99.70	—	—	—	—
Ex-MCR	6.67	71.20	96.80	66.53	93.60	40.31	77.20
Naïve	1.14	2.90	8.45	0.81	8.95	3.32	30.52
COX [†]	1.26	2.00	10.00	4.05	13.70	2.84	26.68
TextME	5.80	77.25	96.85	70.86	92.14	42.15	77.89
PPR (%)	62.2	90.7	99.1	104.6	102.3	99.9	100.9

Notably, TextME achieves PPR exceeding 100% on 3D classification benchmarks (ModelNet40: 104.6%, ScanObjectNN: 99.9%), demonstrating that text-only training can sometimes improve upon pretrained encoder performance. Top-5 preservation consistently exceeds Top-1, indicating that approximate categorical boundaries are well-preserved even when precise rankings differ.

C. Implementation Details

C.1. Model Architecture

Each projection network P_m is implemented as a 2-layer MLP with GeLU activation:

$$P_m(x) = W_2 \cdot \text{GeLU}(W_1 \cdot x + b_1) + b_2 \quad (6)$$

where the hidden dimension matches the source encoder’s embedding dimension d_m , and the output dimension is fixed at $d_h = 2560$ to match Qwen3-Embedding. Total trainable parameters per modality: $\sim 10M$.

C.2. Training Configuration

Table 11. Training hyperparameters. All projection networks are trained with the same configuration across modalities.

Hyperparameter	Value
Batch size	512
Optimizer	AdamW ($\beta_1 = 0.9, \beta_2 = 0.999$)
Weight decay	0.01
Learning rate	5×10^{-4}
LR schedule	Cosine annealing
Training epochs	50
Temperature τ	0.07
Hard negative range	$[0.1 \cdot s_i, 0.9 \cdot s_i]$
Precision	fp16

C.3. Offset Computation

For each modality, we compute centroids using 5,000 randomly sampled text-modal pairs. Table 12 summarizes the datasets used for offset estimation across all evaluated encoders.

Table 12. Datasets used for offset computation. For each encoder, centroids are estimated using 5,000 randomly sampled text-modal pairs from the listed datasets.

Encoder	Modality	Offset Dataset	Domain
CLIP	Image	COCO (Lin et al., 2014)	Natural images
ViCLIP	Video	MSRVTT (Xu et al., 2016)	Web videos
CLAP	Audio	AudioCaps (Kim et al., 2019)	Audio events
Uni3D	3D	Objaverse (Deitke et al., 2023)	Synthetic objects
CXR-CLIP	X-ray	CheXpert (Irvin et al., 2019)	Medical imaging
MoleculeSTM	Molecule	PubChem (Kim et al., 2025)	Chemical compounds
LanguageBind	Text	COCO (Lin et al., 2014)	Natural images

Text inputs are tokenized with a maximum sequence length of 77 tokens. Offsets are pre-computed once and remain fixed throughout training.

We note that the choice of dataset for offset computation may influence both the estimated gap properties and downstream performance. Since the modality gap is computed as the difference between text and modal centroids, the semantic distribution of the offset dataset could affect the resulting offset vector. For instance, encoders whose offset datasets closely match the evaluation domain may exhibit more favorable gap properties, while domain mismatch between offset computation and downstream evaluation could introduce additional variability. Although our experiments demonstrate robust performance across diverse benchmarks, a systematic investigation of how offset dataset selection affects alignment quality remains an important direction for future work.

C.4. Computational Resources

All experiments are conducted on a single NVIDIA A6000 GPU (48GB). Training time averages 2 hours per modality with peak memory usage of approximately 8GB.

D. COX Baseline Implementation

Since the original COX (Huang et al., 2025) codebase is not publicly available, we re-implemented the method following the paper specifications with adaptations for our zero-shot evaluation setting.

Architecture. We employ Vision Transformer Tiny (ViT-T/16) as the encoder backbone with 12 layers, 3 attention heads, and embedding dimension 192. Following the original design, we incorporate a Variational Information Bottleneck (VIB)

layer with stochastic dimensionality reduction to 256 dimensions.

Training Protocol. We follow the two-stage methodology: (1) supervised pre-training on labeled target data for 10 epochs, and (2) information bottleneck fine-tuning for 50 epochs. We use batch size 256, Adam optimizer with learning rate 1×10^{-3} and weight decay 1×10^{-5} .

Key Difference from TextME. COX requires labeled target modality data ($\sim 10K$ samples), trains encoders from scratch ($> 300M$ parameters), and demands architectural alignment between source and target encoders. In contrast, TextME leverages pre-trained encoders with only text descriptions, requires merely $\sim 10M$ trainable parameters, and imposes no architectural constraints.

E. Additional Ablation Studies

E.1. Sample Size for Offset Estimation

We investigate sensitivity to the number of samples used for computing centering offsets.

Table 13. Impact of sample size for offset estimation. Performance remains stable for $N \geq 1,000$.

# Samples	Audio R@1	3D Top-1	Mol. MRR	Rel. Perf.
100	14.91	70.66	34.75	90%
500	14.77	70.58	33.05	95%
1,000	14.89	70.62	36.44	97%
5,000 (default)	15.35	70.86	34.75	100%
10,000	14.95	70.58	32.20	100%

Results demonstrate that offset estimation is robust to sample size, with performance plateauing between 1,000–10,000 samples. Even with only 100 samples, the method achieves 90% of default performance, validating the efficiency of our approach.

E.2. Offset Noise Sensitivity

To assess robustness to offset estimation errors, we perturb the pre-computed offset Δ with additive Gaussian noise: $\Delta' = \Delta + \mathcal{N}(0, \sigma^2 I)$.

Table 14. Offset noise sensitivity. Text→Audio retrieval (R@1), 3D classification (Top-1), and Text→Molecule retrieval (MRR) are reported. Performance degrades gracefully for $\sigma < 0.05$.

Noise σ	Audio R@1	3D Top-1	Mol. MRR
0.000	14.95	70.46	27.97
0.001	14.95	70.30	24.58
0.01	15.04	67.50	22.88
0.05	14.93	34.32	17.80
0.10	14.25	14.91	11.02

Audio demonstrates remarkable stability, maintaining near-baseline performance even at $\sigma = 0.10$. In contrast, 3D and Molecule show sharper degradation at $\sigma \geq 0.05$, indicating these modalities require more precise offset estimation. For practical deployment, 5,000 samples provide sufficient precision with empirical standard error well below $\sigma = 0.01$.